Effect of current type and particle size on wear and corrosion behaviour of electroplated Ni-B₄C composite coatings

S.E. Khadempir[a], B. Lotfi[b]*, Z. Sadeghian[c]

[a] Department of Materials Science and Engineering, Faculty of Engineering, Shahid Chamran University of Ahvaz, 6135473337, Iran, Email: ehsan13_92@yahoo.com

[b] Department of Materials Science and Engineering, Faculty of Engineering, Shahid Chamran University of Ahvaz, 6135473337, Iran, Email: behnaml@scu.ac.ir

[c] Department of Materials Science and Engineering, Faculty of Engineering, Shahid Chamran University of Ahvaz, 6135473337, Iran, Email: z.sadeghian@scu.ac.ir

* Corresponding author

Abstract

Ni-B₄C nanocomposite coatings were deposited onto a pure Cu substrate using electroplating. Different types of current, including direct current (DC), pulse reverse current (PRC), and unipolar pulse current (PC), were applied using various concentrations of micron and nano size particles in the electroplating bath. Microstructure, hardness, and wear and corrosion behavior of the coatings were investigated. Microstructural evaluations were performed using scanning electron microscopy (SEM) and field emission scanning electron microscopy (FESEM). Microhardness, pin-on-disk sliding wear, potentiodynamic polarization, and electrochemical impedance spectroscopy (EIS) tests were conducted on the coatings. Electrodeposition using PRC resulted in a more uniform distribution of co-deposited B₄C microparticles and nanoparticles within the coatings. Nanocomposite coatings reinforced with B₄C nanoparticles were obtained using PRC with a bath concentration of 8 g/l, exhibited higher hardness and improved wear properties compared to composite coatings containing B₄C micron-sized particles. Moreover, using PRC resulted in higher hardness values and improved wear and corrosion resistance compared to PC and DC.

Keywords: electroplating; Ni-B₄C; unipolar pulse current; pulse reverse current

1. Introduction

Electrodeposited composite coatings are fabricated through the addition of ceramic particles to the electrolyte solution. The particles are co-deposited in the metal matrix during the electrical deposition process and provide interesting features depending on the type, volume fraction, and distribution of the particles [1-2]. Uniform distribution of the particles can result in hardness increment, higher wear and corrosion resistance, and enhanced toughness [3-7].

When using ceramic particles known for their hardness, such as Al_2O_3, SiC, WC, TiO_2, and B₄C, a considerable increase in the hardness and wear resistance of composite coatings is expected [8-11]. Among non-oxide ceramics, B₄C and SiC are incredibly important due to their chemical stability, thermal conductivity, and resistance to thermal shock, oxidation, and corrosion [9-10]. B₄C possesses an extremely high hardness (in the range of 2900 to 3580 HV) and high oxidation resistance. For example, recent study indicated that adding -B₄C to electroless Ni–B coatings increased the hardness from ~620 HV to ~870 HV and significantly improved wear resistance. This addition also enhanced the corrosion resistance relative to unreinforced Ni–B coatings [12] .Additionally, it has been reported that the addition of B₄C to coatings can result in higher corrosion resistance [13]. However, according to the literature, the addition of reinforcing particles may result in a reduction in the corrosion resistance of the coatings due to increased surface defects caused by particle agglomeration [14]. Prior studies report that composite coatings with micron-sized particles gain hardness and wear resistance but suffer a "dramatic decrease" in corrosion performance due to particle-related defects [12]. To maximize coating performance, the B₄C contant must be optimized. Moreover, emerging evidence found that Ni–B₄C electroplates achieved the lowest corrosion current at ~6 g/L B₄C in the bath [15]; beyond this level, excessive particle clustering degrades the coating. Using nanoparticles can help alleviate this trade-off: studies on Ni–B electroless coatings show that nano-B₄C not only increases hardness and wear

resistance, but also improves corrosion resistance by filling pores and reducing defects [12]. Thus, controlling particle size and loading is critical for balancing wear and corrosion properties.

Deposition of composite coatings through the electroplating method can be conducted using both direct current (DC) and pulse current (PC). Electroplating using PC can result in the improvement of hardness, ductility, surface roughness, and wear resistance, while also reducing porosity [16-17]. Furthermore, electroplating using PC results in a finer grain structure in the coating because the crystal growth stops during the pulse off-time. In addition, nucleation process is encouraged at the beginning of each pulse period [18].

Through the use of a PC, it is possible to obtain a more uniform distribution of reinforcements throughout the matrix compared to using DC. Although the volume fraction of reinforcing particles in the coating is higher with DC, the hardness and wear resistance are inferior compared to PC. This is related to the heterogeneous distribution of reinforcements in the coating [19]. For example, pulse plating of Ni–SiC or Ni–TiO$_2$ has been shown to yield more homogeneous composites (and higher hardness) than DC plating at the same particle concentration. In short, pulsed plating enhances nucleation and deposit uniformity, boosting hardness and wear resistance while reducing roughness and porosity [20, 21].

Nevertheless, using pulse reverse current (PRC), composite coatings with a higher volume fraction of reinforced particles can be fabricated compared to unipolar pulse current (UPC). The reason for this is that the anode current is applied during the off-time period, and a part of the coating is removed each time [22]. In summary, PRC is expected to outperform both DC and unipolar PC plating by producing Ni–B$_4$C composites with more uniform particle dispersion, lower roughness, and denser microstructure. Such coatings should exhibit superior hardness and wear resistance while avoiding the severe corrosion penalties often seen with simple DC composites. Furthermore, the surface roughness decreases in PRC because the uneven parts of the coating are detached from the surface and re-enter the bath [23]. In summary, PRC is expected to outperform both DC and unipolar PC plating by producing Ni–B$_4$C composites with more uniform particle dispersion, lower roughness, and denser microstructure. Such coatings should exhibit superior hardness and wear resistance while avoiding the severe corrosion penalties often seen with simple DC composites.

The objective is to use various concentrations of micron-sized and nano-sized B$_4$C reinforcing particles were used in an electroplating bath, along with the application of PRC. In addition, the effect of different currents (PRC, PC, and DC) on the microstructure of electrodeposited microcomposite and nanocomposite coatings was investigated. Furthermore, the hardness, wear and corrosion behavior of the resulted coatings were examined, considering an integrative method in comparison with previous studies. By correlating microstructure (e.g. grain size and particle distribution) with measured hardness, wear rate, and corrosion behavior, the interaction of PRC and particle size is clarified. It is expected that PRC will enable higher B$_4$C adding and finer structure than DC or PC, helping to overcome the usual drop in corrosion resistance seen at high particle contents. Through targeted experiments and literature quantification (comparing the evaluated hardness and wear results with reported values [24], the focus is placed on optimization of Ni–B$_4$C nanocomposites for balanced wear and corrosion performance.

2. Experimental procedure
2.1. Electroplating of Ni-B$_4$C coatings

Pure copper sheets of 4 mm × 4 mm × 1 mm dimensions were used as the substrate. One side of the substrate was covered with transparent polyethylene glue for insulation. Before each coating experiment, the copper sheet was grinded under running water using SiC papers (600–2500 grit) to remove surface irregularities and then polished with alumina paste (down to 0.05 μm) to produce a mirror finish. Samples were placed in acetone Merck, ≥99.8%) in an ultrasonic bath for 5 minutes (Elmasonic S 30H ultrasonic bath, 35 kHz) washed with distilled water to remove any sign of oil. Subsequently, samples were dipped into 0.01 molar sulphuric acid for 1 minute and

washed with distilled water to remove any oxide film. Each sample was then immediately dipped into the electroplating bath. The chemical composition of the Watts bath used in the present research is presented in table 1.

Table 1. Electroplating bath composition for composite coating.

Value of SDS/g L^{-1}	Current density/A dm^{-2}	Time/min	Stirrer type	pH	Temp./°C
0.3	6	50	Mechanical & Ultrasonic	4	55
Bath composition			**Concentration/g L^{-1}**		
$NiSO_4.6H_2O$			280		
$NiCl_2.6H_2O$			50		
H_3BO_3			40		
B_4C particles			0-15		
SDS (sodium dodecyl sulfate)			0.3		

B_4C nanoparticles (> 99% purity) with an average diameter of 60 nm and micron-sized B_4C particles (> 99% purity) with an average diameter of 15 μm were used as reinforcements. Fig. 1 shows the morphology of as-received B_4C powders. Ultrasonic agitation and mechanical stirring were applied simultaneously during electrodeposition.

The electrolyte was continuously stirred (Heidolph MR Hei-Standard magnetic stirrer, set at ~500 rpm) and sonicated (Elma Transonic T 470/H, 40 kHz) throughout deposition. In practice, the dispersion stability was monitored by brief visual inspections.

Figure 1. FESEM images of a) Micron size and b) nano size B_4C powder particles

Initial experiments using a DC current density of 6 A/dm² confirmed that a coating with suitable thickness can be obtained after at least 50 minutes. In order to achieve a similar thickness with respect to off-time and reverse pulse period, 58 and 70 minutes were determined as the duration of electrodeposition by PC and PRC, respectively.

Different parameters during electroplating are reported in table 2. All process parameters, including temperature, deposition time, current density, bath pH, surfactant content, and stirring conditions, were kept constant during the electrodeposition of Ni-B_4C composite coatings.

Table 2. Electroplating parameters used for deposition of Ni-B_4C composite coatings.

Value of SDS/g L^{-1}	Current density/A dm^{-2}	Time/min	Stirrer type	pH	Temp./°C
0.3	6	50	Mechanical & Ultrasonic	4	55

Different samples were coated using PRC of 6 A/dm^2 current density with 5, 10, and 15 g/l concentrations of B$_4$C micro-scale particles in the bath. Moreover, 4, 6, 8, and 10 g/l concentrations of B$_4$C nanoparticles were used in the electroplating bath to determine the suitable concentration of B$_4$C nanoparticles for electroplating using PRC. All electrical currents, including PC, PRC, and DC, employed in this study were provided by a rectifier (model SL20PRC) manufactured by IPC Iran. The rectifier is programmable for the PRC currents.

2.2. Microstructure and properties characterization

The electrodeposited coatings were examined by optical microscope (OM, Olympus BX51) to check coverage and thickness, a scanning electron microscope (SEM, LEO 1455VP) and a field emission scanning electron microscope (FESEM, MIRA3 TESCAN) to study microstructure and morphology. The hardness of coatings was determined through microhardness testing (Innova Microhardness Tester) under 50 g loading for a dwell time of 15 seconds. Three distinct zones, including near the coating-substrate interface, mid-point, and near the surface, were considered and an average value was reported as coating hardness.

Wear resistance of Ni-B$_4$C composite coatings was investigated using a pin-on-disk testing machine (Tajhiz Sanat Nasr) following ASTM G99 standard. A heat treated bearing steel of 5 mm diameter, 30 mm height, and 10 mm round tip with a hardness of 60 HRC was chosen as the sliding pin. Dry sliding wear tests were conducted under constant load of 5 N at 100 rpm sliding speed for 400 m. Variations of weight were recorded every 100 m with 0.0001 g precision to calculate the wear rate by dividing the weight loss by distance.

Electrochemical measurements were carried out using a computer-controlled Autolab potentiostat/galvanostat (model AUT 84091) in a conventional three-electrode cell kit. Electrodeposited composite coatings, platinum electrode, and saturated calomel electrode (SCE) were employed as working electrode (WE), counter electrode, and reference electrode, respectively. The WE was covered with transparent polyethylene glue with an exposure area of 1 cm^2. First, the WE was left unpolarized in the test solution (3.5 wt.% NaCl) for 0.5 h to establish a steady state open circuit potential (OCP). Electrochemical impedance spectroscopy (EIS) measurements were then performed at 10 mHz-100 kHz frequency range of OCP with a signal amplitude perturbation of 10 mV peak to peak. Polarization curves were recorded immediately after EIS measurements at a constant sweep rate of 1 mV/s and in the scanning range of -250 mV vs. OCP in order to achieve more positive potentials until the current density exceeded 10 mA/cm^2. All the electrochemical experiments were carried out under quiescent condition at the laboratory temperature (≈25 °C).

3. Results and Discussion

3.1. Microstructural evaluations

Fig. 2 shows the SEM micrographs of the top surface and cross-section of the composite coatings electrodeposited using PRC with 5, 10, and 15 g/l concentrations of B$_4$C microparticles in the electroplating bath. As can be seen, by increasing the concentration of particles in the electroplating bath, the fraction of reinforcing particles in the coating increased. In the coating obtained from the 5 g/l bath concentration, a small number of B$_4$C particles were co-deposited in the coating. Increasing the concentration of B$_4$C particles in the bath up to 10 g/l resulted in an improved distribution of B$_4$C reinforcing particles in the coating (Fig. 2b). As the concentration of B$_4$C particles in the electroplating bath increases, the incorporation of particles into the Ni matrix advances up to an optimal level. Beyond this, excessive concentration leads to particle agglomeration due to increased interparticle collisions and reduced dispersion stability, which results in non-uniform coatings and negatively affects mechanical properties [25]. By increasing

the concentration of reinforcement in the bath up to 15 g/l, the coating exhibited non-uniform distribution of B$_4$C particles, as well as agglomeration and porosity, as shown in Fig. 2c.

Figure 2. SEM micrographs of top surface and cross-section of composite coatings electro-deposited by PRC with different concentrations of a)5, b)10, and c)15 g/l B$_4$C micro particles in electroplating bath

Fig. 3 shows the FESEM micrographs of Ni-B$_4$C$_{(nano)}$ nanocomposite coatings obtained through electrodeposition using PRC with 6, 8, and 10 g/l B$_4$C nanoparticles in the bath. B$_4$C nanoparticles can be observed distributed on the surface of the coatings. Increasing the concentration of nanoparticles from 6 to 8 g/l in the bath has resulted in an increased co-deposition of B$_4$C nanoparticles during electroplating. However, according to Fig. 3c, further increments of B$_4$C concentration in the electroplating bath, up to 10 g/l, resulted in a high tendency for nanoparticles to agglomerate. It has been stated that, by increasing the concentration of nanoparticles beyond an optimum level, particle collision rates increase, leading to the formation of agglomerates with

lower wettability in the electroplating bath. This can result in a non-uniform distribution of particles and the formation of porosity in the electroplated coating [9].

Figure 3. FESEM micrographs of the surface and cross-section of Ni-B$_4$C$_{(nano)}$ nanocomposite coatings obtained from electro-deposition by PRC with different concentrations of a) 6, b)8, and c)10 g/l B$_4$C nanoparticles in electroplating bath

Fig. 4 shows the results of microhardness measurements of micron-scale and nano-scale Ni-B$_4$C composite coatings obtained from various particle concentrations in the electroplating bath. By increasing the concentration of B$_4$C micron-size particles in the electroplating bath (up to 10 g/l), the hardness of Ni-B$_4$C composite coatings increased. Further increase in the B$_4$C content led to a reduction in hardness. This can be attributed to the agglomeration of reinforcing particles and the formation of porosity throughout the coating, as revealed in Fig. 2. The presence of hard ceramic B$_4$C particles reinforces the Ni matrix by multiple mechanisms. Primarily, the Orowan

dispersion strengthening mechanism operates: dislocations bow and loop around fine, non-

shearable B₄C particles, raising the stress required for plastic deformation [26]. In addition, the nanoparticles refine the Ni grain structure (Hall–Petch effect) and carry load themselves, all of which enhance hardness[27] . Likewise, increasing the concentration of B₄C nanoparticles up to 8 g/l resulted in an increase in the hardness of nanocomposite coatings. This can be attributed to the distribution of reinforcing particles within the Ni matrix and the Orowan dispersion hardening effect [20, 29].

Increasing the concentration of B₄C nanoparticles from 8 to 10 g/l resulted in a decrease in hardness value. Further increasing the concentration of nanoparticles beyond a critical limit has been reported by researchers to decrease the hardness due to particle agglomeration [30].

Increased co-deposition of B₄C nanoparticles with higher particle concentrations in the electroplating bath can be explained by Guglielmi's two-step absorption model. According to this model, higher concentrations of particles in the bath result in an increased absorption rate inside the electrolyte and, consequently, an increment of the reinforcement phase in the coating [1, 31]. As illustrated by the results, it can be concluded that the optimal concentration levels of micron-sized and nano-sized B₄C particles in the electroplating bath using PRC are 10 g/l and 8 g/l, respectively.

Figure 4. Micro-hardness values of a) Ni-B₄C(micron) composite coatings and b) Ni-B₄C(nano) nanocomposite coatings, obtained from different particle concentrations in electroplating bath

To investigate the effect of current type on electrodeposition process, composite coatings with 10 g/l B₄C(micron) particles and nanocomposite coatings with 8 g/l B₄C(nano) nanoparticles in the bath were deposited using PC, PRC, and DC.

Fig. 5 shows the SEM micrographs of the surface and cross-section of Ni-B$_4$C$_{(micron)}$ (10 g/l) composite coatings obtained using various current types. As can be seen, the composite coating obtained through electroplating using PRC showed the most uniform distribution of co-deposited B$_4$C particles with the least surface roughness compared to other current types. In the coating obtained using PC, a higher rate of fine B$_4$C particles is noticeable compared to that electroplated using DC. However, PC resulted in the lowest content of co-deposited particles in the coating among the studied current types. Moreover, the use of DC resulted in more reinforcing particles of larger size in the matrix and the roughest surface finish. Applying a monotone current during electroplating can cause the entrance of both bulky and fine particles without selective priority, which results in surface roughness. Similar results have been reported by other researchers [30, 32].
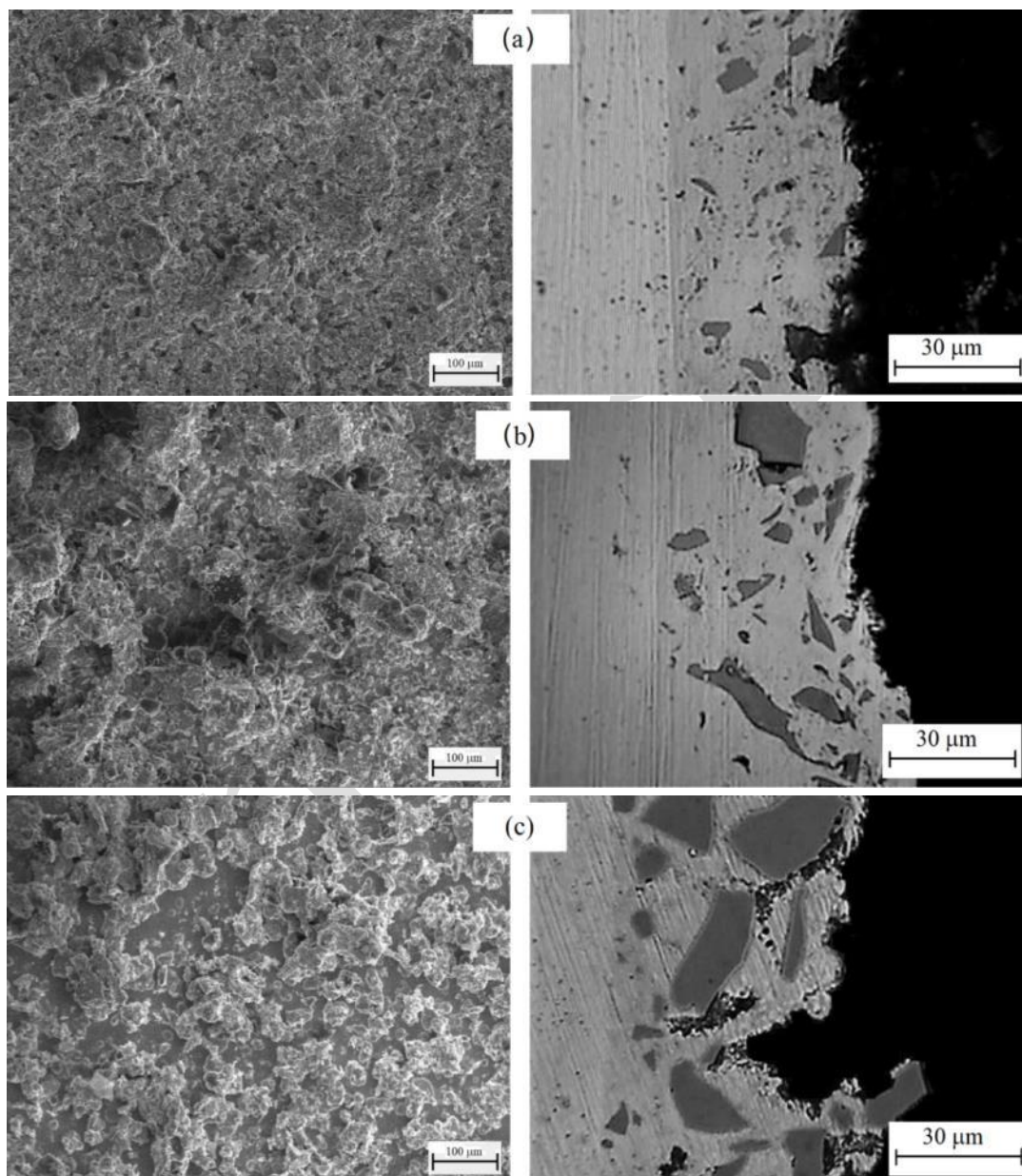

Figure 5. Top surface and cross-section SEM micrographs of Ni-B$_4$C$_{(micron)}$ (10 g/l) composite coatings obtained from various current

In the presence of anodic current during PRC, bulky particles may detach from the surface of the coating and re-enter the bath. Anodic current can also result in the detachment of the matrix

material. As a consequence, higher fraction of fine reinforcing particles as well as low surface roughness can be achieved in the coatings obtained through PRC compared to PC and DC current types as seen in Fig. 5. In other words, by using PRC, blackout time prevents the entrance of large particles and agglomerates into the coating, repeatedly [30, 32].

Fig. 6 illustrates the FESEM micrographs of the surface and cross-section of Ni-B$_4$C$_{(nano)}$ (8 g/l) nanocomposite coatings obtained through electroplating using various current types. As can be seen, by using PRC during electroplating, a relatively uniform distribution of nanoparticles has been co-deposited in the coating.

Figure 6. FESEM micrographs of the surface and cross-section of Ni-B$_4$C$_{(nano)}$ (8 g/l) nano composite coatings obtained from various current types; a) PRC, b) PC and c) DC

Using PC and DC current types has resulted in the agglomeration of some nanoparticles as depicted in Fig. 6b and c. In addition, electroplating using PRC produced a smoother surface in

comparison to other current types. The smoother surface of PRC coatings arises because the reverse pulses inhibit uncontrolled dendritic growth and coarse particle deposition. In agreement, it is noted that dispersing nanoparticles uniformly leads to finer crystallites and a smoother morphology[33]. It has been reported that the use of PC causes an increase in electrocrystallization rather than enhancement of the mass transport on the cathode surface [34]. This effect together with selective deposition of finer particles, which can be considered as heterogeneous nucleation sites, cause competitive rates of nucleation and growth resulting in a smoother surface. Moreover, with the use of DC the precipitation rate of Ni ions increases that causes a more globular surface containing porosities and cracks.

The results of microhardness measurement on microcomposite and nanocomposite coatings obtained using various current types are presented in Fig. 7. As was expected, both Ni-B$_4$C coatings containing micron-scale particles and nanoparticles obtained using PRC exhibited the highest hardness. Higher hardness values obtained by PRC can be attributed to the enhanced co-deposition and uniform distribution of particles as well as lower agglomeration. The use of DC resulted in the least hardness in both microcomposite and nanocomposite coatings, which can be attributed to the agglomeration of particles within the matrix and higher porosity content.

Figure 7. Micro-hardness values of a) Ni-B$_4$C$_{(micron)}$ (10 gr/lit) composite coatings and b) Ni-B$_4$C$_{(nano)}$ (8 gr/lit) nanocomposite coatings, obtained from various current types

3.2. Wear and corrosion behaviour

Fig. 8 demonstrates the wear weight loss after different sliding distances for Ni-B$_4$C

microcomposites and nanocomposites obtained through electroplating using PRC, PC, and DC current types. The Ni-B$_4$C microcomposite coating fabricated using PRC exhibited the lowest weight loss after 400 m of sliding distance among microcomposite coatings. This improvement mirrors the hardness results: higher hardness and better particle distribution yield better protection. Ceramic B$_4$C particles in the Ni matrix act as a load-bearing phase and reduce plastic deformation at contact points[35]. Furthermore, the composite coating obtained using DC showed the highest weight loss at the same sliding distance.

As seen in Fig. 5c, a combination of very large B$_4$C particles together with finer particles co-deposited simultaneously during electroplating using DC. In addition, electroplating using DC resulted in noticeable agglomeration of B$_4$C particles and increased roughness. It is evident that the existence of hard ceramic particles enhances wear resistance. Moreover, lower surface roughness of the coating is expected to result in improved wear resistance [36]. Ceramic reinforcement particles cause a reduction in plastic deformation at the contact area with the pin and reduction in adhesive contact due to higher hardness results in improvement of wear properties. This phenomenon can occur when a uniform distribution without particle agglomeration is achieved [37]. As previously mentioned, by using PRC, surface roughness decreased and a more uniform distribution of reinforcement particles was achieved compared to PC and DC current types.
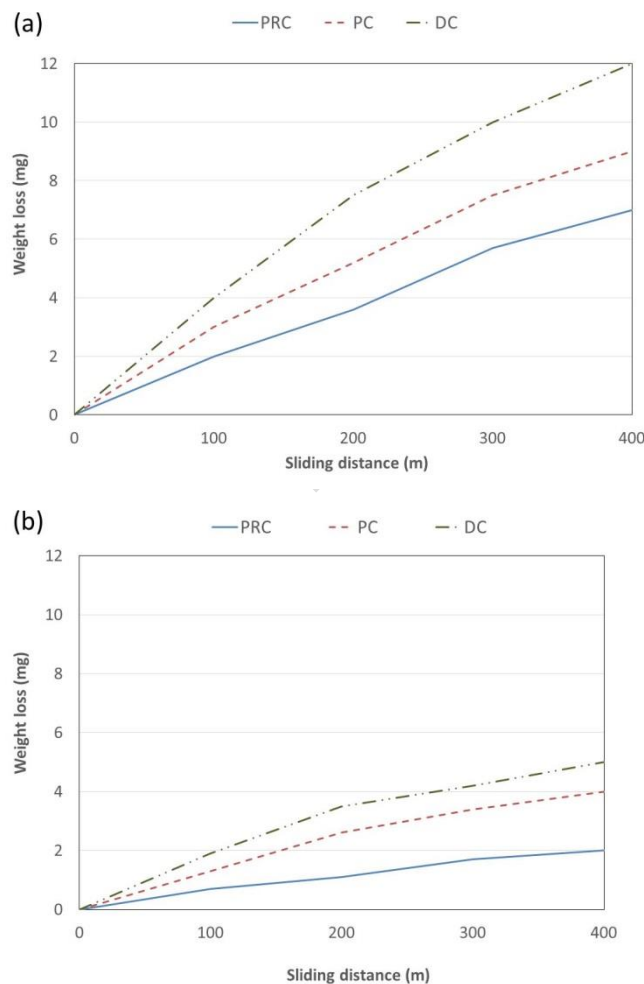

Figure 8. Weight loss curves attained from the wear tests on a) Ni-B$_4$C$_{(micron)}$ (10 gr/lit) composite coatings and b) Ni-B$_4$C$_{(nano)}$ (8 gr/lit) nanocomposite coatings, obtained from various current types

Fig. 9 shows the SEM micrographs of the worn surfaces of microcomposite and nanocomposite coatings electroplated using different current types. The worn surface of the coating produced

using PRC exhibited very few wave-like lines. By comparing the worn surfaces, it can be concluded that the magnitude of damage on the surface of the coatings was less when using PC compared to DC and the least weight loss was obtained by using PRC. The PC coatings show shallower grooves with some torn debris (mixed adhesive-abrasive wear). Both micro and nano Ni-B$_4$C composite coatings fabricated using DC demonstrated discontinuous wear tracks consisting of deep grooves as well as ploughing and noticeable hollowness, which can be considered as signs of severe adhesion and ploughing abrasion (Fig. 9e and f). In fact, these coatings show adhesive wear to be the major wear mechanism. On the worn surface of Ni-B$_4$C composite coatings produced using PC, less wave-like lines and shallower grooves with fewer detachments can be seen. Furthermore, more continuous grooves are observable due to higher abrasive wear. Therefore, signs of both adhesive and abrasive wear can be observed in these coatings (Fig. 9c and d).

Figure 9. SEM morphologies of worn surfaces of a), c), e) Ni-B$_4$C$_{(micron)}$ (10 g/l) and b), d), f) Ni-B$_4$C$_{(nano)}$ (8 g/l) coatings obtained from various current types (arrows show the direction of sliding of the pin)

As previously mentioned, electroplating with the use of DC resulted in rougher surfaces in both microcomposite and nanocomposite coatings with mostly larger particles. With the movement of

the pin on the surface, hard B_4C particles are detached from the matrix and move between the coating and the pin. It has been stated that in metal matrix composites, abrasive wear increases with increase in the size of co-deposited particles [38, 39]. Moreover, increasing surface roughness and surface porosity has been shown to result in the reduction of wear resistance [40]. In summary, the superior wear resistance of PRC coatings can be attributed to their higher hardness, uniform particle reinforcement, and lower surface roughness [33, 35].

Experimental impedance results of Ni-B_4C composite coatings in 3.5 wt.% NaCl solution are displayed in Fig. 10. Both micro and nano Ni-B_4C composite coatings obtained using PRC showed higher corrosion resistance and the diameter of the semicircle in Nyquist plots decreased in order of PRC > PC > DC. The observation of a single depressed semicircle in the Nyquist plots indicates that the corrosion reaction is only controlled by the charge-transfer process [41].

The deviation from an ideal semicircle, i.e., with a centre below the real axis, is mostly attributed to frequency dispersion resulted from surface roughness/inhomogeneity [42]. Bode plots show the existence of an equivalent circuit containing a single constant phase element related to the charge transfer process in the interface region of metal/solution. The increase of the impedance at low frequencies in the Bode plot corresponds to the higher corrosion resistance. The ZSimpWin software was used to determine the impedance parameters from the experimental results.
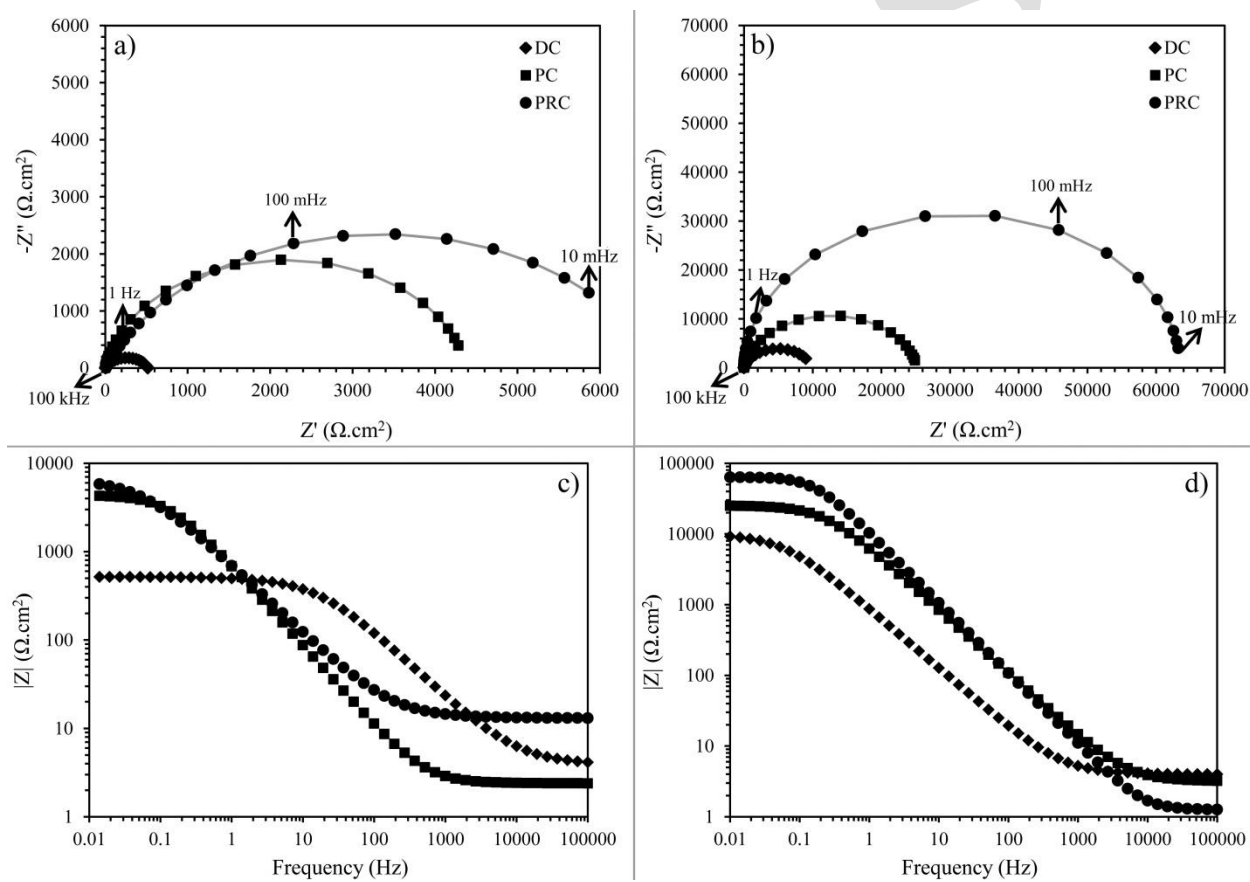

Fig. 10. Nyquist diagrams (a, b) and bode plots (c, d) of the micro (a, c) and nano (b, d) Ni-B_4C composite coatings in 3.5 wt.% NaCl solution

Fig. 11 shows the electrical equivalent circuit with chi-squared of less than 10^{-8}, which is a combination of polarization resistance (R_p), and Q, the constant phase element (CPE), both in series with uncompensated solution resistance (R_s). These electrochemical parameters are summarized in tables 1 and 2. In this case, due to the surface heterogeneity at a micro-level or nano-level, such as surface roughness/porosity or diffusion, CPE is applied for more fitting

accuracy instead of an ideal capacitor [42-44]. The impedance function of CPE is mathematically expressed by Eq. (1) [41].

$$Z_{CPE} = Y_0^{-1}(j\omega)^{-n} \tag{1}$$

Where, Y_0 is the magnitude of the CPE, $\omega = 2\pi f$ is the angular frequency at the maximum value of the imaginary part of the impedance spectrum, and n is phase shift, which represents deviation from ideal behaviour.
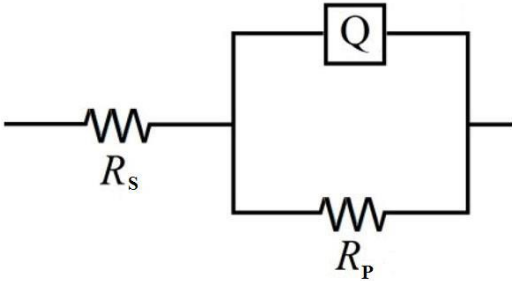

Fig. 11. Equivalent electrical circuit model used to fit obtained experimental data from EIS measurement

Electrochemical impedance parameters for Ni-B$_4$C microcomposite and nanocomposite coatings in 3.5 wt.% NaCl solution are presented in tables 3 and 4. It can also be observed that in both micro and nano Ni-B$_4$C composite coatings, the values of R$_p$ of the coatings decreased in order of PRC > PC > DC and the values of Q (CPE of electrical double layer) decreased in order of DC > PC > PRC . However, in all current types, the nanocomposite coating showed a higher corrosion resistance than the microcomposite coating.

Table 3. Electrochemical impedance parameters for micro Ni-B4C composite coatings in 3.5 wt.% NaCl solution

Current type	R_s (Ω cm^2)	Q		R_p (Ω cm^2)
		Y_0($\mu\Omega^{-1}$s^{n}cm^{-2})	n	
DC	3.9	335	0.77	515
PC	2.4	266	0.81	4376
PRC	13	53	0.78	6699

Table 4. Electrochemical impedance parameters for nano Ni-B4C composite coatings in 3.5 wt.% NaCl solution

Current type	R_s (Ω cm^2)	Q		R_p (Ω cm^2)
		Y_0($\mu\Omega^{-1}$s^{n}cm^{-2})	n	
DC	4.0	239	0.84	9913
PC	3.2	29	0.89	25260
PRC	1.3	15	0.90	63550

Potentiodynamic polarization curves of Ni-B$_4$C composite coatings in 3.5 wt.% NaCl solution are presented in Fig. 12. An extended pseudo-passive region can be observed in the anodic branches, especially in nano Ni-B$_4$C composite coating. The electrochemical parameters, such as corrosion potential (E$_{corr}$), cathodic and anodic Tafel slopes (β_c and β_a), and corrosion current density (i$_{corr}$) obtained by extrapolation of the Tafel lines [35], are given in tables 5 and 6. Both micro and nano Ni-B$_4$C composite coatings showed decreased corrosion current (i$_{corr}$) in order of PRC > PC > DC, which shows a good correlation with the EIS measurements. Ni-B$_4$C$_{(nano)}$ composite coating presented a greater decrease in i$_{corr}$ compared to Ni-B$_4$C$_{(micro)}$ composite coating.
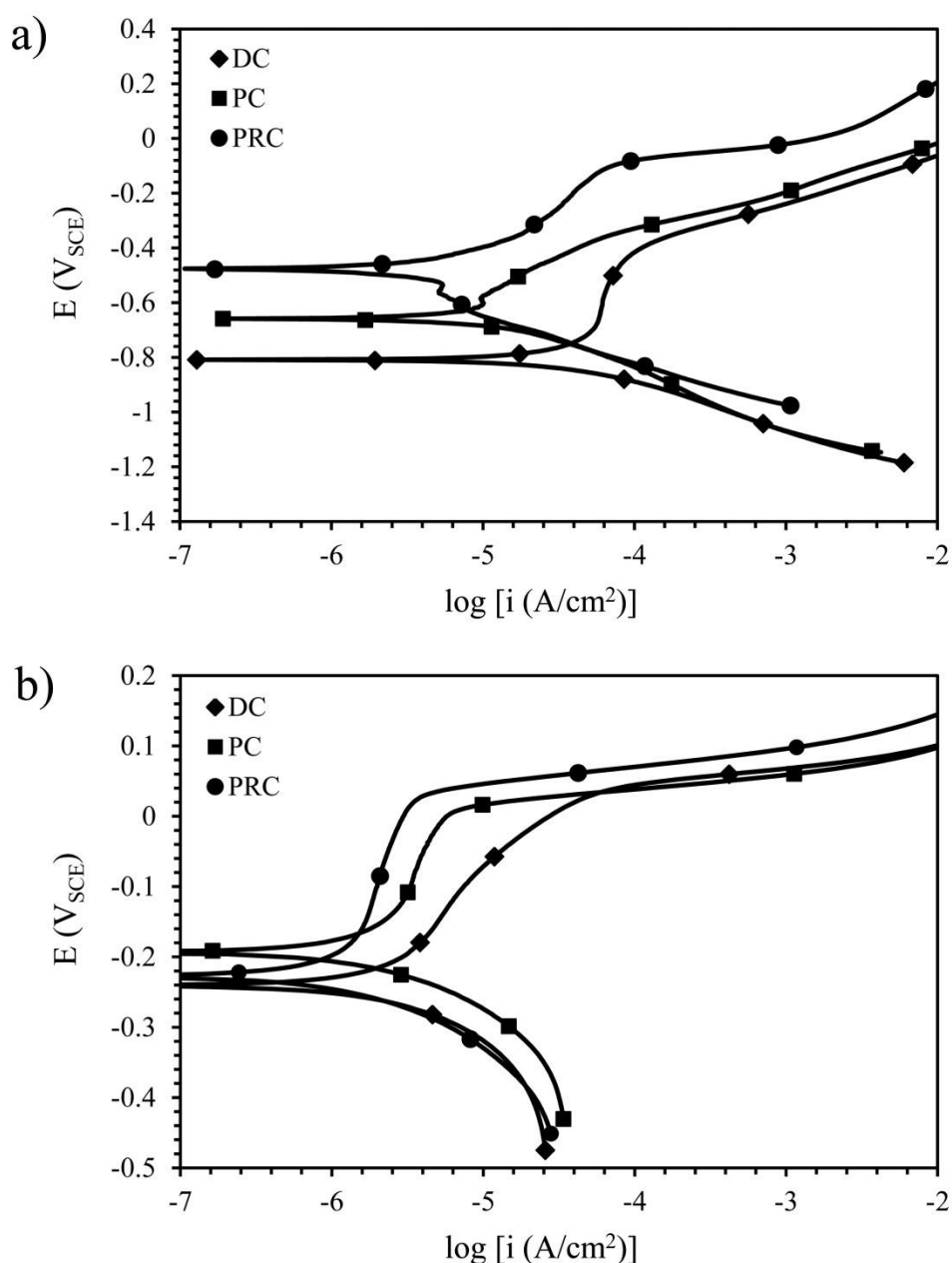
Fig. 12. Potentiodynamic polarization curves of (a) Ni-B$_4$C$_{(micro)}$, and (b) Ni-B$_4$C$_{(nano)}$ composite coatings in 3.5wt.% NaCl solution

Table 5. Electrochemical kinetic parameters of Ni-B$_4$C$_{(micro)}$ composite coatings electroplated by different current types extracted from the polarization experiment in 3.5 wt.% NaCl solution.

Current type	I_{corr} (μA cm^{-2})	E_{corr} (mV$_{SCE}$)	β_a (mVdec^{-1})	B_c (mVdec^{-1})
DC	3.44	-808.72	24.5510	27.4220
PC	1.02	-659.38	17.3800	25.0400
PRC	0.32	-477.09	19.2730	19.6030

Table 6. Electrochemical kinetic parameters of Ni-B$_4$C$_{(nano)}$ composite coatings electroplated by different current types extracted from the polarization experiment in 3.5 wt.% NaCl solution.

Current type	I_{corr} (nA cm^{-2})	E_{corr} (mV$_{SCE}$)	β_a (mVdec^{-1})	B_c (mVdec^{-1})
DC	112.90	-241.23	8.37240	8.96100
PC	150.76	-193.48	14.4610	17.0810
PRC	53.14	-227.36	9.17440	8.53650

Several factors such as imposed current type, particle size, uniform distribution of particles, filling of the micro holes, and submicron defects can affect the corrosion resistance of composite coatings. Electrodeposition is usually associated with submicron and micron porosities. It has been reported that B_4C nano-sized particles can fill the defects more effectively than micron-sized particles, and thereby, improve the corrosion resistance of the coating [36]. Furthermore, improvement of corrosion properties of Ni-B_4C composite coatings electroplated by PRC, compared to PC and DC, can be attributed to the reduction of surface roughness and more uniform distribution of reinforcing particles.

Regarding the above discussions, the highest corrosion resistance that is assigned to Ni-$B_4C_{(nano)}$ nanocomposite coating was produced through PRC electroplating and can be related to several interrelated microstructural parameters. In addition, extended pseudo-passive region in Ni-$B_4C_{(nano)}$ nanocomposite coating may be explained by improved co-deposition of B_4C particles in the Ni matrix and filling of the electrodeposition defects.

4. Conclusions

(1) By using 10 g/l of micron-sized and 8 g/l of nano-sized B_4C particles in the electroplating bath, uniform distribution of B_4C particles was achieved in the coatings.

(2) Lower concentration resulted in inadequate co-deposition of the particles and higher concentration caused agglomeration of the particles. Moreover, using 15 g/l of B_4C microparticles in the bath increased the porosities.

(3) By using PRC for electroplating of Ni-B_4C, surface roughness decreased and a more uniform distribution of reinforcing particles and enhanced hardness were achieved compared to PC and DC.

(4) Ni-$B_4C_{(nano)}$ (8 g/l) coating electroplated using PRC exhibited the highest hardness value and the lowest weight loss.

(5) The weight loss of the Ni-$B_4C_{(nano)}$ (8 g/l) coating electroplated using PRC was 40% lower than that electroplated using DC. A similar comparison between microcomposite coatings revealed this value to be 58%.

(6) Regardless of the size of B_4C reinforcing particles, the dominant wear mechanism in the coatings electrodeposited using PRC and DC was abrasive and adhesive, respectively, and both abrasive and adhesive wear mechanisms were found in the coatings produced using PC.

(7) Using PRC resulted in higher corrosion resistance in both micro and nano Ni-B_4C composite coatings.

(8) The highest corrosion resistance was achieved in Ni-$B_4C_{(nano)}$ nanocomposite coating produced through PRC electroplating due to the reduction of surface roughness and defects and a more uniform distribution of nanoparticles.

References

[1] Hovestad, A., Janssen, L.J.J. *"Electrochemical codeposition of inert particles in a metallic matrix". J. Appl. Electrochem.*, 1995, 25, 519–527. https://doi.org/10.1007/BF00573209

[2] Walsh F.C. and Larson C., *"Towards improved electroplating of metal-particle composite coatings." T I Met Finis.*, 2020, 98(6), 288-299, doi.org/10.1080/00202967. 2020.1819022.

[3] Hu, F. and K.C. Chan, *"Equivalent circuit modelling of Ni–SiC electrodeposition under ramp-up and ramp-down waveforms." Mater. Chem. Phys.*, 2006, 99(2), 424-430. doi.org/10.1016/j.matchemphys.2005.11.015

[4] Szczygieł, B. and M. Kołodziej, *"Composite Ni/Al$_2$O$_3$ coatings and their corrosion resistance." Electrochim. Acta.*, 2005, 50(20), 4188-4195. doi.org/10.1016/j.electacta. 2005.01.040

[5] Lampke, T.,Wielage, B., Dietrich, D. and Leopold, A., "*Details of crystalline growth in co-deposited electroplated nickel films with hard (nano)particles.*" *Appl. Surf. Sci.*, 2006, 253(5), 2399-2408. doi.org/10.1016/j.apsusc.2006.04.060.

[6] Ger, M. D., *"Electrochemical deposition of nickel/SiC composites in the presence of surfactants.*" *Mater. Chem. Phys.*, 2004, 87(1), 67-74. doi.org/10.1016/j.matchemphys.2004.04.022.

[7] Ünal, E. and İ.H. Karahan, *"Production and characterization of electrodeposited Ni-B/hBN composite coatings."* *Surf. Coat. Tech.*, 2018, 333, 125-137. doi.org/10.1016/j.surfcoat.2017.11.016.

[8] Aruna, S. T. and Srinivas, G., *"Wear and corrosion resistant properties of electrodeposited Ni composite coating containing Al$_2$O$_3$–TiO$_2$ composite powder." Surf. Eng.*, 2015, 31(9), 708-713. doi.org/10.1179/1743294415Y.0000000050

[9] Wang, P., Cheng, Y. and Zhang, Z., *"A study on the electrocodeposition processes and properties of Ni–SiC nanocomposite coatings." J. Coat. Technol. Res.*, 2011, 8(3), 409-417. doi.org/10.1007/s11998-010-9310-1.

[10] He, T., He, Y., Li, H. and Su, Z., *"Fabrication of Ni-W-B$_4$C composite coatings and evaluation of its micro-hardness and corrosion resistance properties." Ceram. Int.*, 2018. 44(8), 9188-9193. doi.org/10.1016/j.ceramint.2018.02.128.

[11] Lin, C.S., Le, C.Y., Chang, C.F. and Chang, C.H., *"Annealing behavior of electrodeposited Ni-TiO$_2$ composite coatings." Surf. Coat. Tech.*, 2006, 200(12), 3690-3697. doi.org/10.1016/j.surfcoat. 2004.10.001.

[12] Rezagholizadeh M., Ghaderi M., Heidary A., Monirvaghefi S.M., "*The Effect of B4C Nanoparticles on the Corrosion and Tribological Behavior of Electroless Ni-B-B4C Composite Coatings"*, Электронная обработка материалов, 2015, 51(1), 19–25.

[13] Paydar, S., Jafari, A., Bahrololom,M.E. and Mozafari, V., *"Influence of BN and B$_4$C particulates on wear and corrosion resistance of electroplated nickel matrix composite coatings." Tribol. Mater. Surf. Interface.*, 2015, 9(2), 105-110. doi.org/10.1179/1751584X15Y.0000000007.

[14] Shen, L., Fan, M., Zhao, K., Qiu, M. and Tian, Z., *"Preparation and properties of nanocomposite coatings on sintered NdFeB magnets." Mater. Res. Express*, 2018, 5(8), 086401. doi.org/1088/2053-1591/aad121.

[15] Jiang, Ji Bo, Wei Dong Liu, Lei Zhang, Qing Dong Zhong, Yi Wang, and Qiong Yu Zhou. "*Electrodeposition and Hardness and Corrosion Resistance Propertie of Ni/Nano-B4C Composite Coatings.*" *Adv. Mater. Res.* 2011, 399–401, 2055–60. doi.org/10.4028/www.scientific.net/amr.399-401.2055.

[16] Wang, Q.W., Huang, J.L., Liu, J.N., Yang, Y.F., Han, G.F. and Li, W., *"Enhanced performance of electrodeposited Ni-SiC plating as an alternative to electroplated chromium deposits: the effect of pulse duty cycle." Surf. Topog. Metrol. Prop.*, 2022, 10(1), 015024. doi.org/ 10.1088/2051-672X/ac5503.

[17] Song J., He, Y., Li, H., Zhang, Y., Liu, B., Song, R., Zhang, Z. and He, Y., *"Preparation of pulse electrodeposited Ni-B/ZrC composite coatings and investigation of their mechanical properties and corrosion resistance." Surf. Coat. Tech.*, 2022, 447, 128845. doi.org/10.1016/j.surfcoat.2022.128845.

[18]   Chen, C.Y., Yoshiba, M., Nagoshi, T., Chang, T.M., Yamane, D., Machida, K., Masu, K. and Sone, M. *"Pulse electroplating of ultra-fine grained Au films with high compressive strength." Electrochem. Commun.*, 2016, 67, 51-54. doi.org/10.1016/j.elecom.2016.03.017.

[19]   Hou, K.-H., Hwu, W.-H., Ke, S.-T and Ger, M.-D., *"Ni–P–SiC composite produced by pulse and direct current plating." Mater. Chem. Phy.*, 2006, 100(1), 54-59. doi.org/10.1016/j.matchemphys. 2005.12.016.

[20]   Zimmerman, A., Clark, D., Aust, K., Erb, U., *"Pulse electrodeposition of Ni–SiC nanocomposite." Mater. Lett.*, 2002. 52. 85-90. doi.org/10.1016/S0167-577X(01)00371-8.

[21] Yılmaz, G., Hapçı, G., Orhan, G. *"Properties of Ni/Nano-TiO₂ Composite Coatings Prepared by Direct and Pulse Current Electroplating." J. Mater. Eng. Perform.*, 2015, 24, 709–720. doi.org/10.1007/s11665-014-1346-4

[22]   Garcia, I., Conde, A., Langelaaan, G., Fransaer, J. and Celis, J.P., *"Improved corrosion resistance through microstructural modifications induced by codepositing SiC-particles with electrolytic nickel." Corros. Sci.*, 2003,   45(6),   1173-1189.   doi.org/10.1016/S0010-938X(02)00220-2.

[23]   Pavlatou, E.A., Ispas, A., Leisner, P. and Zanella, C., *"Hardening effect induced by incorporation of SiC particles in nickel electrodeposits." J. Appl. Electrochem.*, 2005, 36(4), 385-394. doi.org/10.1007/s10800-005-9082-y

[24] Lampke Th, Leopold, A., Dietrich D., Alisch G., WielageB., "*Correlation between structure and corrosion behaviour of nickel dispersion coatings containing ceramic particles of different sizes*". *Surf. Coat. Tech.* 2006, 201, 3510-3517. doi.org/10.1016/j.surfcoat.2006.08.073.

[25] Gül H, Kılıç F, Uysal M, Aslan S, Alp A, Akbulut H**.** *"Effect of particle concentration on the structure and tribological properties of submicron particle SiC reinforced Ni metal matrix composite (MMC) coatings produced by electrodeposition*". *Appl. Surf. Sci.* 2012;258(10):4260–4267. doi: 10.1016/j.apsusc.2011.12.069

[26] Cui, A., Wang, X. & Cui, Y. "Multiscale modelling of precipitation hardening: a review. *J Mater. Sci: Mater. Theory*, 2024, 8, 13. doi.org/10.1186/s41313-024-00066-6

[27] Armstrong, R. W. *"Hall–Petch description of nanopolycrystalline Cu, Ni and Al strength levels and strain rate sensitivities." Philos. Mag.*, 2016, 96(29), 1-12. 10.1080/14786435.2016.1225168.

[28]   Shi, L., Sun, C., Gao, P., Zhou, F. and Liu, W., *"Mechanical properties and wear and corrosion resistance of electrodeposited Ni–Co/SiC nanocomposite coating." Appl. Surf. Sci.*, 2006, 252(10), 3591-3599. doi.org/10.1016/j.apsusc.2005.05.035.

[29]   Wu, Y.T., Lei, L., Shen, B. and Hu, W.B., *"Investigation in electroless Ni–P–Cg(graphite)–SiC composite coating." Surf. Coat. Tech.*, 2006, 201(1), 441-445. doi.org/10.1016/j.surfcoat. 2005.11.140.

[30]   Low, C.T.J., Wills, R.G.A., and Walsh, F.C., *"Electrodeposition of composite coatings containing nanoparticles in a metal deposit." Surf. Coat. Tech.*, 2006, 201(1), 371-383. doi.org/10.1016/j.surfcoat.2005.11.123.

[31]   Mohajeri, S., Dolati, A. and Rezagholibeiki, S. *"Electrodeposition of Ni/WC nano composite in sulfate solution." Mater. Chem. Phys.*, 2011, 129(3), 746-750.

[32]   Podlaha, E.J., *"Selective Electrodeposition of Nanoparticulates into Metal Matrices." Nano Lett.*, 2001, 1(8), 413-416. doi.org/10.1016/j.matchemphys.2011.04.053.

[33] Rao H, Li W, Zhao F, Song Y, Liu H, Zhu L, Chen H. *"Electrodeposition of High-Quality Ni/SiC Composite Coatings by Using Binary Non-Ionic Surfactants", Molecules*, 2023, 10;28(8), 3344. doi: 10.3390/molecules28083344. PMID: 37110578; PMCID: PMC10144436.

[34]   Erb, U., Aust, K.T. and Palumbo, G., *Electrodeposited Nanocrystalline Metals, Alloys, and Composites*, in book: Nanostructured Materials (Second Edition), ed. C.C. Koch, William Andrew Publishing: Norwich, NY, 2007, 235-292, doi.org/10.1016/B978-081551534-0.50008-7.

[35] Pinate, S., Ghassemali, E., Zanella, C *"Strengthening mechanisms and wear behavior of electrodeposited Ni–SiC nanocomposite coatings*". *J. Mater. Sci.*, 2022, 57, 16632–16648. https://doi.org/10.1007/s10853-022-07655-1

[36]   Góral, A., L. Lityńska-Dobrzyńska, and M. Kot, *"Effect of Surface Roughness and Structure Features on Tribological Properties of Electrodeposited Nanocrystalline Ni and Ni/Al₂O₃ Coatings." J. Mater. Eng. Perform*., 2017, 26(5), 2118-2128, doi.org/10.1007/s11665-017-2662-2.

[37]   Dehgahi, S., Amini, R. and Alizadeh, M., *"Corrosion, passivation and wear behaviors of electrodeposited Ni–Al₂O₃–SiC nano-composite coatings." Surf. Coat. Tech.,* 2016, 304, 502-511. doi.org/10.1016/j.surfcoat.2016.07.007

[38]   Gyawali, G., Joshi, B., Tripathi, K. and Lee, S.W., *"Effect of ultrasonic nanocrystal surface modification on properties of electrodeposited Ni and Ni-SiC composite coatings." J. Mater. Eng. Perform.*, 2017, 26(9), 4462-4469. doi.org/10.1007/s11665-017-2662-2.

[39]   Nieto, A., Yang, H., Jiang, L. and Schoenung, J.M., *"Reinforcement size effects on the abrasive wear of boron carbide reinforced aluminum composites." Wear*, 2017, 390-391, 228-235. doi.org/10.1016/j.wear. 2017.08.002.

[40]   Chen, L., Wang, L., Zeng, Z. and Zhang, J., *"Effect of surfactant on the electrodeposition and wear resistance of Ni–Al₂O₃ composite coatings." Mater. Sci. Eng. A*, 2006, 434(1), 319-325. doi.org/10.1016/j.msea.2006.06.098.

[41]   Erami, R.S.,Amirnasr, M., Meghdadi, S. and Talebian, M., *"Carboxamide derivatives as new corrosion inhibitors for mild steel protection in hydrochloric acid solution." Corros. Sci.*, 2019, 151, 190-197. doi.org/10.1016/j.corsci. 2019.02.019.

[42]   Salarvand, Z., Amirnasr, M, Talebian, M., Raeissi, K. and Meghdadi, S., *"Enhanced corrosion resistance of mild steel in 1 M HCl solution by trace amount of 2-phenyl-benzothiazole derivatives: Experimental, quantum chemical calculations and molecular dynamics (MD) simulation studies." Corros. Sci*., 2017, 114, 133-145. doi.org/10.1016/j.corsci.2016.11.002.

[43]   Mert, B.D., Yuce, A.O., Kardas, G. and Yazici, B., *"Inhibition effect of 2-amino-4-methylpyridine on mild steel corrosion: experimental and theoretical investigation." Corros. Sci.*, 2014, 85, 287-295. doi.org/10.1016/j.corsci.2014.04.032.

[44]   Chevalier, M., Robert, F., Amusant, N., Traisnel, M., Roos, C. and Lebrini, M., *"Enhanced corrosion resistance of mild steel in 1 M hydrochloric acid solution by alkaloids extract from Aniba rosaeodora plant: Electrochemical, phytochemical and XPS studies."Electrochim. Acta*, 2014, 131, 96-105. doi.org/10.1016/j.electacta. 2013.12.023.

[45]   McCafferty, E., *"Validation of corrosion rates measured by the Tafel extrapolation method", Corros. Sci*., 2005, 47(12), 3202-3215. doi.org/10.1016/j.corsci. 2005.05.046.

[46]   Bakhit, B. and Akbari, A. *"Effect of particle size and co-deposition technique on hardness and corrosion properties of Ni–Co/SiC composite coatings" Surf. Coat. Tech.*, 2012, 206(23), 4964-4975. doi.org/10.1016/j.surfcoat.2012.05.122.